



University of
Massachusetts
Amherst

SEX SPECIFIC ELECTROPHYSIOLOGY OF AROMATASE NEURONS IN THE MEDIAL AMYGDALA

Item Type	Thesis (Open Access)
Authors	Correia, Marcelo Henrique
DOI	10.7275/14350640
Download date	2026-06-12 23:31:18
Link to Item	https://hdl.handle.net/20.500.14394/33881

Sex Specific Electrophysiology of Aromatase Neurons in the Medial Amygdala

A Thesis Presented

By

MARCELO HENRIQUE CORREIA

Submitted to the graduate school of the
University of Massachusetts Amherst in partial fulfillment
of the requirements for the degree of

MASTER OF SCIENCE

SEPTEMBER 2019

Neuroscience and Behavior

Sex Specific Electrophysiology of Aromatase Neurons in the Medial Amygdala

A Thesis Presented

By

MARCELO HENRIQUE CORREIA

Approved as to style and content by:

Joseph F. Bergan, Chair

Geng-Lin Li, Member

Luke Ramage-Healey, Member

Paul S. Katz, Graduate Program Director
Neuroscience & Behavior Program

ACKNOWLEDGMENTS

I thank God for giving me health, strength, courage and determination during this journey to fight and overcome the obstacles of life.

I thank my mother, Nadir Correia, who always excelled in my education and encouraged me to continue my academic career. His struggle to overcome obstacles in life motivates me and makes me proud. Thank you for always being there and I'm very happy for that. I also thank my father Amilton Correia, who, even though he is not present among us, is still a source of pride to me. Your encouragement for my study drives me to this day and I am very grateful to him, thank you very much. Thanks also to my brothers Silvana Cristina Correia L. Alencar and Anderson César Correia who always believed in me and cheered for my success.

I would like to thank my advisor Dr. Joe Bergan for believing me. I also thank you for your patience in counseling and for the help and encouragement of this Master's degree. To my co-counselor Dr. GengLin Li for the conversations, for the help in the technique and analysis of electrophysiology and the sharing of ideas, thank you very much. To Dr. Luke Ramage-Healey for his advice and guidance during the process of this master's degree.

I would like to thank to the Graduate Program in Neuroscience and Behavior, for the opportunity to live with extraordinary people, for having provided means for this walk to have been more pleasant and for the opportunity to take the master's degree. I would also like to thank the people who worked in the laboratory, where I learned how to be a scientist and improve my scientific and intellectual skills: Dani Frolov, Hwang Fuu-jiun,

Adolfo Ernie Cuadra, Prakruti Nanda, Tal Inbar, Joe Dwyer, Jonathan Woodson. I would like to thank my classmates: Jessica Caballero, Sarah Winokur, Helena Jacob and Nicole Lee. Thank you for every encouragement during this walk, thank you for making my days in Amherst better days and thank you for allowing me to live with such valiant people as you.

Thank you very much for the family I have created in and out of the ones, people who will be forever present in my thoughts, my thanks: Matheus Macedo-Lima, Beata Kamińska-Kordowska, Andrea Silva Gotay, Deniz Besik and Ilker Emrah Ozay.

ABSTRACT

SEX SPECIFIC ELECTROPHYSIOLOGY OF AROMATASE NEURONS IN THE

MEDIAL AMYGDALA

SEPTEMBER 2019

MARCELO HENRIQUE CORREIA, B.S., UNIVERSIDADE ESTADUAL DE

MARINGÁ

M.S., UNIVERSITY OF MASSACHUSETTS AMHERST

Directed by: Joseph Bergan

The medial amygdala (MeA) is a central node in the interwoven circuits that regulate social behavior based on pheromones. Aromatase-expressing (arom^+) neurons in the MeA are key for the establishment and maintenance of sex differences. Here, we characterized the intrinsic electrophysiological properties of arom^+ neurons and non-aromatase (arom^-) neurons in the MeA of male and female mice. Most electrophysiological properties were similar for arom^+ neurons in the MeA between sexes, but the relative refractory period was twice as large in female mice. We also show that the firing pattern and firing frequency is markedly different between arom^+ and arom^- neurons. The activity of MeA neurons could be modulated by estradiol, which reduced activity in arom^+ neurons in males. The differences between arom^+ and arom^- neurons were observed in both sexes suggesting that aromatase expression delineates a neural population in the MeA with similar and unique electrophysiological properties.

TABLE OF CONTENTES

	Page
ACKNOWLEDGMENTS	iii
ABSTRACT.....	iv
LIST OF FIGURES	vii
CHAPTER	
1. INTRODUCTION	1
2. MATERIALS AND METHODS.....	4
2.1 Animals	4
2.2 Brain dissection.....	4
2.3 Electrophysiology and analysis.....	5
2.4 Immunostaining	6
2.5 Data analysis	7
3. RESULTS	8
3.1 Anatomy	8
3.2 Electrophysiology	9
3.3 Estradiol activity on arom ⁺ neurons.....	14
4. DISCUSSION.....	16
BIBLIOGRAPHY.....	19

LIST OF FIGURES

Figure	Page
1. Photomicrography of arom^+ and arom^- neurons	8
2. Map of neurons recorded from the MeA	9
3. Arom^+ neurons firing pattern	10
4. After hyperpolarization score for arom^+ neurons in male and female animals	10
5. Number of spikes by current in arom^+ neurons in the MeA of male and female mice	11
6. Arom^+ and arom^- neurons firing pattern in female	12
7. Number of spikes by current in arom^+ and arom^- neurons in the MeA of female mice.....	12
8. Arom^+ and arom^- neurons firing pattern in male	13
9. Number of spikes by current in arom^+ and arom^- neurons in the MeA male mice..	14
10. Estradiol activity on arom^+ neurons in the MeA in males	15
11. Estradiol activity on arom^+ neurons in the MeA across time	15

CHAPTER 1

INTRODUCTION

Successful social interactions enhance an animal's chances of survival and their chances of passing genes to the next generation. Likely because of their importance for survival, neural circuits that mediate efficient reproductive, parental, and defensive behaviors are highly conserved. Adjustments to this core circuitry bestow the specific repertoires of social behaviors inherent to each species. Just as songs allow birds to attract mates and establish territory, chemical cues mediate social behaviors in mice.

Chemical signals are detected by the vomeronasal organ (VNO) which sends projections to the accessory olfactory bulb (AOB) which, in turn, projects directly to the MeA (Scalia and Winans, 1975; Kang, et. al, 2011). The medial amygdala (MeA) is a central node of circuits that regulate social behavior in mice (Unger, et. al, 2015; Bergan, et. al, 2014; Yao, et. al, 2017). Outputs from the MeA target areas including the hypothalamus which control innate behaviors and homeostatic functions in mice (Newman, 1999; Pardo-Bellver, et. al, 2012).

The MeA mediates social behaviors including: mating, fighting and parenting (Meredith and Westberry, 2004; Dielenberg et. al, 2001), as well as, asocial behaviors like self-grooming (Hong et. al, 2014). Distinct social behaviors are associated with different but overlapping subregions of the MeA. For example, activation of the posteroventral medial amygdala (MeApv) is linked to defensive behavior (Choi et al., 2005) while activation of the posterodorsal medial amygdala (MeApd) is more closely associated with reproductive behaviors (Meredith and Westberry, 2004). Optogenetic activation of GABAergic cells in the MeApd generates aggressive behavior while

activation of glutamatergic neurons generates self-grooming (Hong et. al, 2014). Inactivating arom^+ neurons in the MeA using inhibitory designer receptors exclusively activated by designer drugs (DREADDs) resulted in a delay in aggression in both male and female (Unger et. al, 2015). In addition, oxytocin signaling through arom^+ neurons in the MeA alters social behavior and the neural representation of social stimuli in the MeA (Yao et al., 2017).

Anatomical differences between males and females have been observed in many brain regions associated with social behavior. The first observed sex difference in the anatomy of MeA neurons was that the neuronal soma size is smaller in female than in male in squirrel monkeys (Bubenik and Brown, 1973). Subsequent studies showed that the volume of MeApd was smaller in female when compared to male mice (Cooke et al., 1999; Morris et. al, 2008). More recently, the density of projecting fibers from AOB to arom^+ neurons in the MeA was found to be denser in males when compared to females (Niemeyer, unpublished data). These lines of evidence, in accord with known sex differences in MeA sensory responses (Bergan et. al 2014; Yao et. al 2017), suggest that sex differences in the intrinsic properties of MeA neurons may be important mediators of sex-differences in mouse social behavior.

The MeApd contains an abundant number of arom^+ neurons (Yao et. al, 2017). Aromatase is an enzyme that converts testosterone to estradiol and is critical for establishing sex-differences in both neuroanatomy and behavior (Naftolin et. al, 1971; Naftolin et al., 1996; Wu et al., 2009). Testosterone (a precursor for estradiol) influences the volume and neuronal soma size in the MeApd in mice and the MeA is enriched with androgen and estrogen receptors, indicating clear hormonal regulation of the MeA (Sheridan 1979; Yokosuka et. al, 1997; Cooke 1999). Hormones, like estradiol, can have an important effect in how neurons encode chemosensory

information, and it has become increasingly clear that in some systems these effects occur rapidly (Ramage-Healey et al., 2008).

It is presently not known whether the intrinsic properties of arom^+ neurons in the medial amygdala differ between male and female animals. Similarly, it is not clear how estradiol alters intrinsic properties of arom^+ neurons in the MeA, ultimately leading to a change in circuit function. In this study we describe sex differences in the intrinsic properties and hormonal regulation of MeA arom^+ neurons in the context of social behavior.

Given that arom^+ neurons in the MeA are essential for establishing and maintaining sex differences in social behavior, we hypothesize that the circuit-level properties that support sex-differences in behavior will manifest in differences in the input-output relationship of arom^+ neurons and/or hormone-dependent modulation of arom^+ neurons in the MeA by estradiol. Understanding how those neurons process information at the single-cell level will provide insights as to how social behavior is mediated by the underlying neural circuits and how the same neural circuit can mediate different behaviors in response to the same stimulus depending on an animal's sex, age, and hormonal state.

To test our hypothesis, we generated mice that express the fluorescent protein tdTomato in arom^+ cells, which allowed us to target arom^+ neurons in the MeA directly. We then studied the electrophysiological properties of arom^+ neurons in the MeA using whole-cell patch clamp. We believe these experiments provide new insight into how this neural circuit mediates social behavior in males and females; with a long-term goal of understanding how cellular and circuit-level sex differences in social circuits may impact brain functions in humans during sickness and health.

CHAPTER 2

MATERIALS AND METHODS

2.1 Animals

All mice were maintained in light-dark cycles of 12 hours each cycle, with *ad libitum* access to food and water. All animals were treated according to the animal protocol reviewed and approved by the IACUC of the University of Massachusetts - Amherst.

For the following experiments we used Aro:cre \times tdTomato male and female mice between 2-4 months old. To generate those mice, Cyp19a1(aromatase)-Cre BAC transgenic line (Yao, et. al, 2017) was bred with a homozygous Rosa26-lsl-tdTomato reporter line (Madisen, et. al, 2010) that was purchased from Jackson Labs (Bar Harbor, Maine). This transgenic reporter line has a LoxP-flanked Stop locus that prevents the transcription of a red fluorescent protein, in this case tdTomato. When the LoxP-flanked Stop line is crossed into the ARO:cre line, all aromatase cells that contain cre express tdTomato fluorescence.

2.2 Brain dissection

For brain slice experiments, mice were deeply anesthetized with isoflurane and then quickly decapitated. The brains were rapidly removed and placed in ice-cold (bubbling 95% O₂/5% CO₂) CO₂ solution containing the following (in mM): 89.1 sucrose, 13.88 glucose, 87.27 NaCl, NaHCO₃, 2.5 KCl, 7 MgCl₂ · 6H₂O, 0.37 CaCl₂, and 1.25 NaH₂PO₄ · H₂O. Coronal slices (300 μ m thick) were prepared using a vibratome (Leica VT1200S) and incubated at 35 °C for 30 min in artificial oxygenated cerebrospinal fluid (ACSF) containing the following (in mM): NaCl, 25

glucose, 25 NaHCO₃, 2.5 KCl, 1.325 MgCl₂, 2.5 CaCl₂ and 1.2 NaH₂PO₄ · H₂O. After 30 minutes at room temperature, the slices were transferred to the recording chamber.

2.3 Electrophysiology and analysis

Slices were perfused with oxygenated ACSF and maintained at room temperature. Recording electrodes were made with borosilicate glass (8-12 MΩ) drawn from a vertical pipette extractor (PC-10, Narishige, Tokyo, Japan) and filled with an internal solution containing the following (in mM): 20 KCl, 120 KGlu, 0.1 CaCl₂, 5 EGTA, 5 HEPES, 3 MgATP, 0.5 NaGTP (pH 7.3 with KOH, 290 mOsm). Neurobiotin (0.1%) was added to the internal solution to fill patched cells. In the estradiol modulation experiments, estradiol (50 nM) was added to the external solution.

Patch-clamp recordings were done at room temperature (22°C) with a Heka amplifier (EPC10/2, Heka, Lambrecht / Pfalz, Germany). After achieving whole-cell configuration, voltage was clamped at -80 mV, and a “soft” current clamp switch was performed in which the current used to hold the cell at -80 mV was maintained. Neurons were then depolarized by injecting current. The voltage signals were low-pass filtered at 2 kHz and sampled at 100 kHz. Whole cell patch-clamp was made from arom⁺ and arom⁻ in the medial amygdala (MeA) using infrared differential contrast (DIC) coupled to a microscope (BX51WIF, Olympus, Tokyo, Japan) with a 60X water immersion lens equipped with fluorescence accessories.

Electrophysiological experiments measured: 1) The maximum frequency of spikes; 2) The frequency of spikes at the resting membrane potential; 3) The voltage threshold for eliciting an action potential (rheobase); 4) The latency of action potential initiation; 5) The input resistance of the cell.

For determining the maximum spiking frequency, eleven 500-ms current steps starting at 20 pA increasing in 20 pA steps were used. We counted the maximum number of action potentials observed in any condition. During the resting membrane potential frequency spikes protocol, we injected zero current and recorded for one second.

For determining the action potential voltage threshold and action potential timing threshold we injected current until 200 pA during 1 second. The threshold and action potential latency were manually measured. For the voltage threshold we measured the voltage where the cell start to fire an action potential and we also counted the time in milliseconds when the cell start to fire an action potential.

For determining the input resistance, eleven 200-ms current steps starting at -50 pA increased by 10pA were used. To analyze the input resistance we used the Ohm's law: $R = V / I$, where R is the resistance, V is the voltage and I is the current. Data analysis was performed in Igor Pro 6.0 software (WaveMetrics).

2.4 Immunostaining

After recordings, slices were drop-fixed in 4% paraformaldehyde (PFA) for two hours. After that, tissue was washed in PBS-Triton 0.1% for three times for 15 minute each time. Streptavidin was used in the concentration 1:200 (DyLight 649 Streptavidin - Vector Laboratories). After one hour, sections were then washed three times in PBS-Triton 0.1% for 10 minutes each. Finally, sections were mounted with mounting media (1:10 – PBS and Glycerol) and coverslipped. The images were then

collected using the microscope BX51WIF (Olympus, Tokyo, Japan) and analyzed with Image J.

2.5 Data analysis

Images and electrophysiological data were further analyzed with custom MATLAB (Mathworks, Natick, MA, United States) scripts. Briefly, these scripts allowed the electrophysiological properties to be directly compared to the location, morphology, and expression pattern of each recorded neurons. We also used MATLAB to perform the analysis in the raw data and to generate graphs.

CHAPTER 3

RESULTS

3.1 Anatomy

Arom⁺ neurons were identified in the MeA using conditional tdTomato expression in arom⁺ (Fig. 1). Arom⁺ neurons fluoresced bright red (Fig. 1A). Patched neurons were filled with neurobiotin and visualized in far-red after streptavidin tagging (Fig. 1B). This allowed us to distinguish arom⁺ neurons (arrow) from arom⁻ neurons (arrowhead) during slice recordings (Fig. 1 A-C). The location of each recorded neuron was determined and mapped onto a standard atlas of the mouse MeA (Fig 2; Male: blue dots; female: red dots). Each representative dot corresponds to a specific cell and is referenced with information about the cellular morphology, aromatase expression, and animal identity for that cell (Fig. 2 A – B).

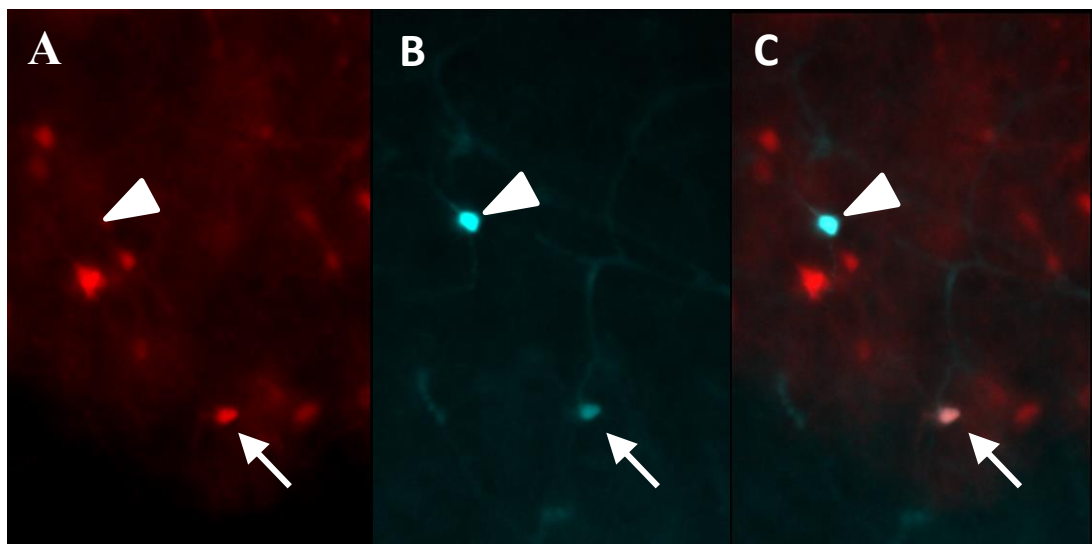


Figure 1. Photomicrography of arom⁺ and arom⁻ neurons. A) Aromatase expressing neurons are shown in red. B) Filled neurons with neurobiotin-streptavidin conjugate is shown in cyan. C) Merged channels from panel A and B are shown. Arrowhead = non-aromatase neuron; Arrow = aromatase-expressing neuron.

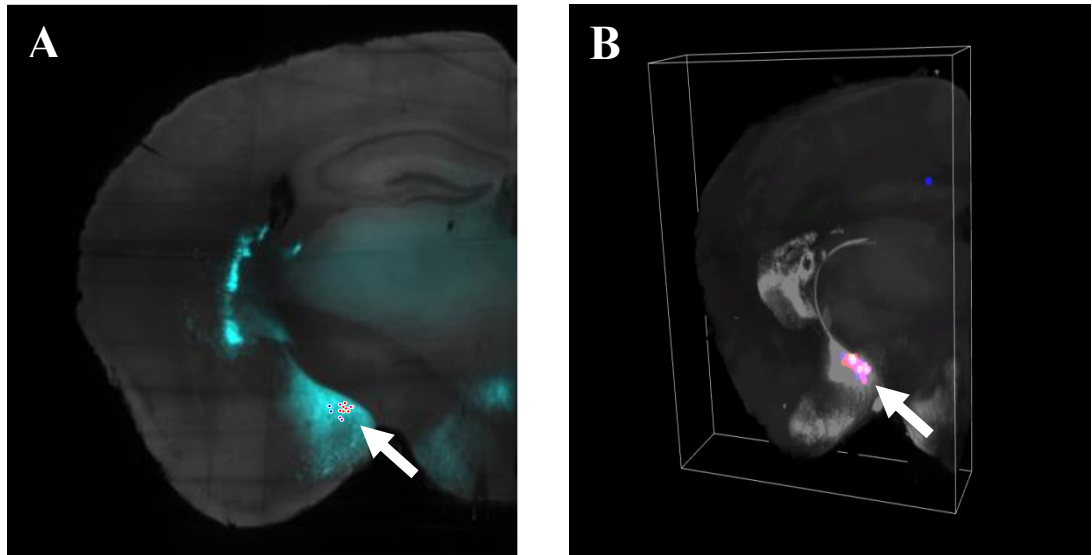


Figure 2. Map of neurons recorded from the MeA. A) Coronal view of a representative section with selected data points. B) 3D image representation of the recorded neurons in the MeA. Male: blue dots; female: red dots). Each dot represents a specific data in Matlab. Arrow= MeA.

3.2 Electrophysiology

We measured electrophysiological properties in $arom^+$ and $arom^-$ in both male and female mice. Measured properties include: maximum frequency of spikes, resting membrane potential frequency of spikes, action potential voltage threshold, action potential timing threshold, and input resistance. None of the above parameters showed a significant difference for MeA neurons recorded in males versus females (Fig. 3 A and C; t-test, maximum frequency of spikes $p=0.37$; resting membrane potential frequency of spikes $p= 0.85$; action potential voltage threshold $p= 0.43$; action potential timing threshold $p=0.40$, and input resistance $p=0.37$). The same depolarization current step stimulus was used for all cells regardless of animal sex or aromatase expression (Fig. 3 B and D). The maximum frequency of spikes in $arom^+$ neurons in male was 1.88 spikes and in $arom^+$ neurons in female were 2.31 spikes when we applied the current step stimulus. When the $arom^+$ neurons were at rest we obtained 4.85 spikes in males and 4.47 spikes in females. From the same

representative Fig. 3 the action potential voltage threshold for male was -46.8 mV and for female was -48.2 mV, while the action potential timing threshold was 0.37 s for male and 0.36 for female. The input resistance was 729 MOhm for male arom^+ neurons and 664 MOhm for female arom^+ neurons.

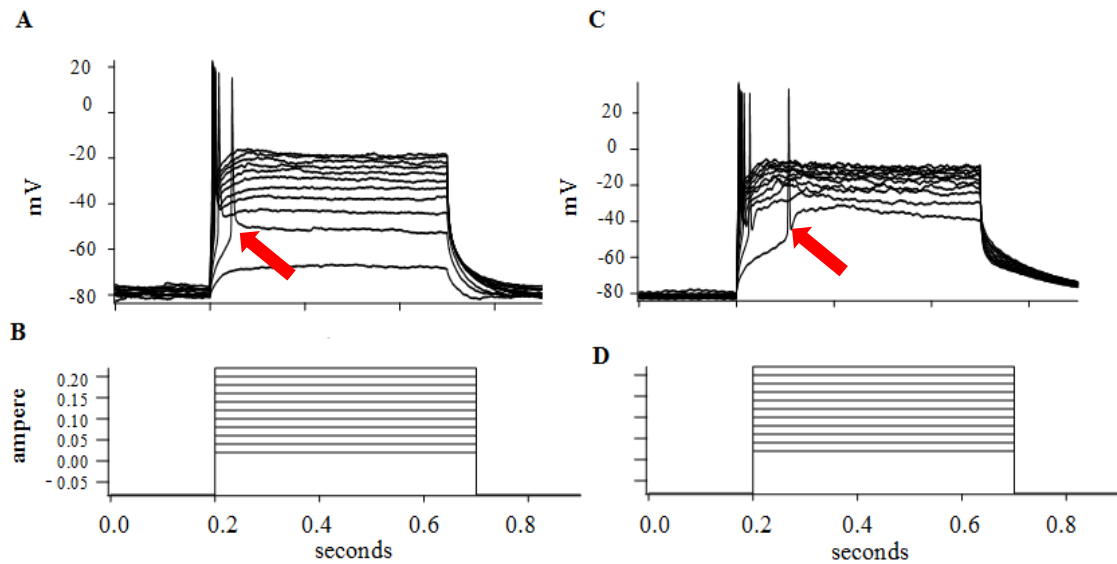


Figure 3. Arom^+ neurons firing pattern. A) Firing pattern of arom^+ neurons in male in response to the current step stimulus. B;D) Current step stimulus - eleven current steps with an increase of 20pA for each step during 500ms . C) Firing pattern of arom^+ in female in response to the current stimulus. Red arrow shows relative refractory period.

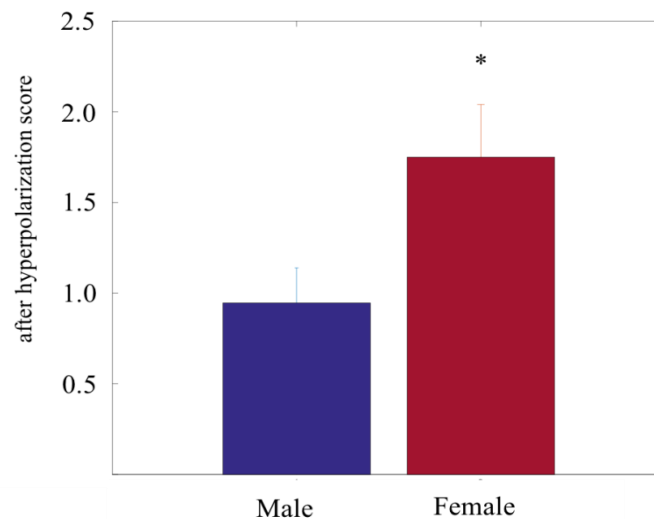


Figure 4. After hyperpolarization score for arom^+ neurons in male and female animals. The after hyperpolarization was larger and more sustained in female mice than in male mice (Male: Mean: 0.946 ± 0.196 , Blue; Female: Mean: 1.75 ± 0.294 , Red). * $p=0.024$ (ttest)

The relative refractory period in arom^+ neurons was roughly twice as large in arom^+ from female as compared to male mice (Fig. 4 female arom^+ neurons the relative refractory period had a mean of 1.75 (after hyperpolarization score) and arom^+ neurons in male this mean was 0.94 (Fig. 3A,C; Fig. 4; $p=0.024$).

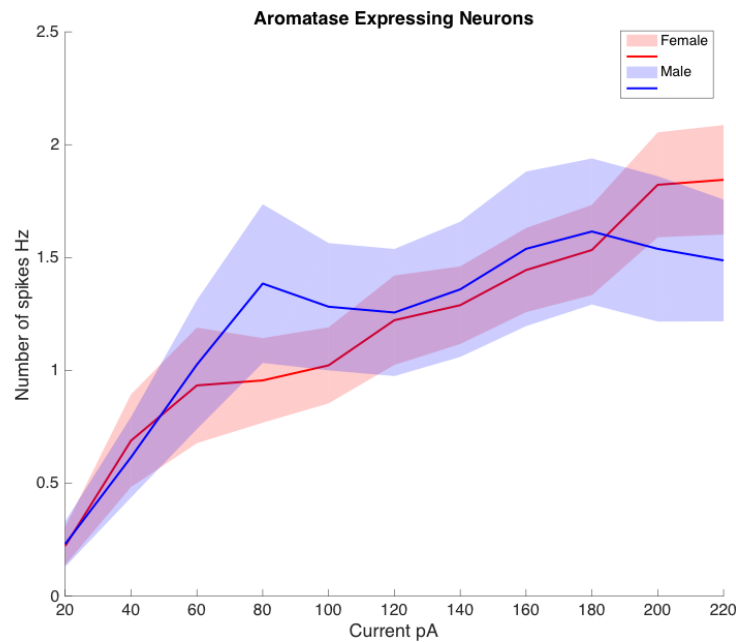


Figure 5. Number of spikes by current in arom^+ neurons in the MeA of male and female mice. Dark blue: number of spikes mean in male; blue shading: SEM. Dark red: number of spikes mean in female; red shading: SEM in female. No statistical difference (ttest).

The number of evoked spikes increased similarly with current steps for both sexes, and no statistically significant differences were observed (Fig. 5, t-test $p>0.05$). When we compared arom^+ with arom^- neurons, we observed a clear difference in the intrinsic properties (Fig. 6). Arom^- neurons (Fig. 6A) fired more frequently than arom^+ neurons (Fig. 6C) in both males and females (t-test, $p<0.05$). This difference was more pronounced in females where the higher firing rate of arom^- neurons was clear for all current steps, with statistical significance for currents of 60, 80 100 and 120pA (Fig. 7; ttest, $p\leq 0.05$). The same depolarization current step stimulus was used for all cells regardless of animal sex or aromatase expression (Fig. 6 B, D).

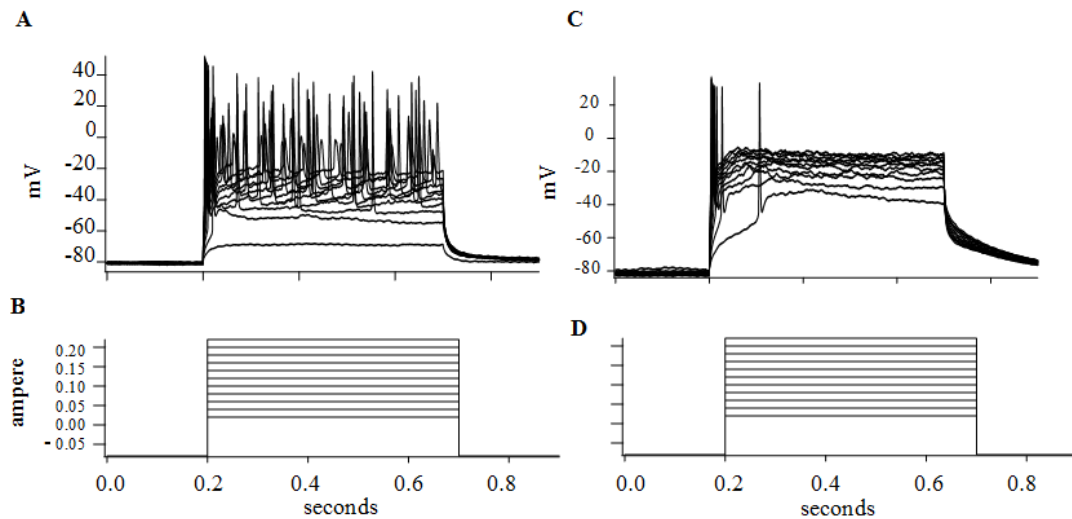


Figure 6. Arom⁺ and arom⁻ neurons firing pattern in female. A) Firing pattern of arom⁻ neurons in female in response to the current step stimulus. B;D) Current step stimulus - eleven current steps with an increase of 20pA for each step during 500ms. C) Firing pattern of arom⁺ neurons in female in response to the current stimulus.

While arom⁺ neurons in both males and females monotonically increased their firing rate with increasing current steps, arom⁻ neurons displayed a peak firing rate with an injected current of 80 pA, followed by a gradual reduction in response to subsequent current steps (Fig. 7).

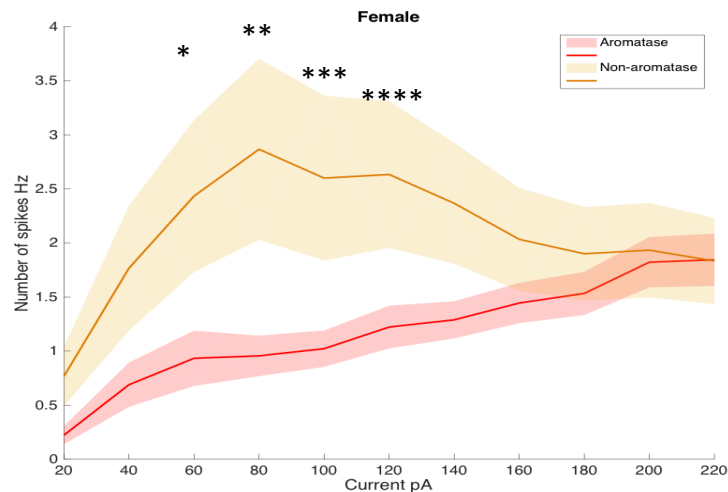


Figure 7. Number of spikes by current in arom⁺ and arom⁻ neurons in the MeA of female mice. Dark red: number of spikes mean in arom⁺ neurons; red shading: SEM. Dark yellow: number of spikes mean in arom⁻ neurons female; yellow shading: SEM in female. ttest
 *p=0.05 – (arom⁺ neurons: mean: 0.933 spikes, SEM= 0.256), (arom⁻ neurons: mean: 2.433 spikes, SEM= 0.702);
 **p=0.03 – (arom⁺ neurons: mean: 0.955 spikes, SEM= 0.187), (arom⁻ neurons: mean: 2.867 spikes, SEM= 0.837);
 ***p=0.05 – (arom⁺ neurons: mean: 1.022 spikes, SEM= 0.168), (arom⁻ neurons: mean: 2.600 spikes, SEM= 0.762);
 ****p=0.05 – (arom⁺ neurons: mean: 1.222 spikes, SEM= 0.198), (arom⁻ neurons: mean: 2.633 spikes, SEM= 0.679).

Analysis of arom^- neurons with arom^+ neurons in the MeA of males also showed a similar pattern as observed in females arom^+ neurons (Fig. 8 A) firing less spikes as compared with arom^- neurons (Fig. 8 C). The same depolarization current step stimulus was used for all cells regardless of animal sex or aromatase expression (Fig. 8 B and 8). In males, arom^- neurons fired more than arom^+ neurons and exhibited a peak firing rate with a current injection of 120 pA, while arom^+ neurons monotonically increased their firing rates (Fig. 9). Arom^+ neurons were statistical different from arom^- neurons at currents of 100 and 120pA (Fig. 9, $p=0.03$).

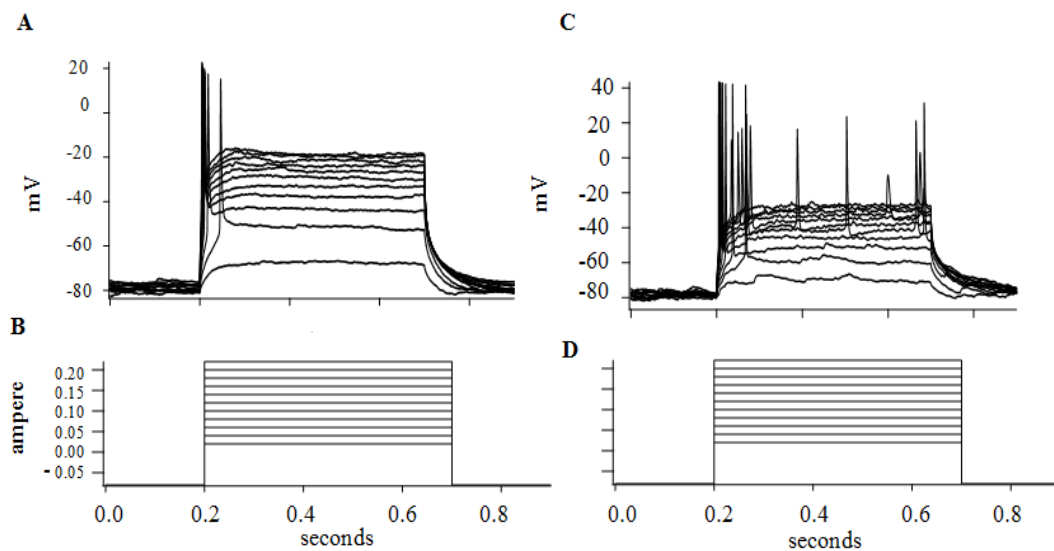


Figure 8. Arom^+ and arom^- neurons firing pattern in male. A) Firing pattern of arom^+ neurons in male in response to the current step stimulus. B;D) Current step stimulus - eleven current steps with an increase of 20pA for each step during 500ms. C) Firing pattern of arom^- neurons in male in response to the current stimulus given in D.

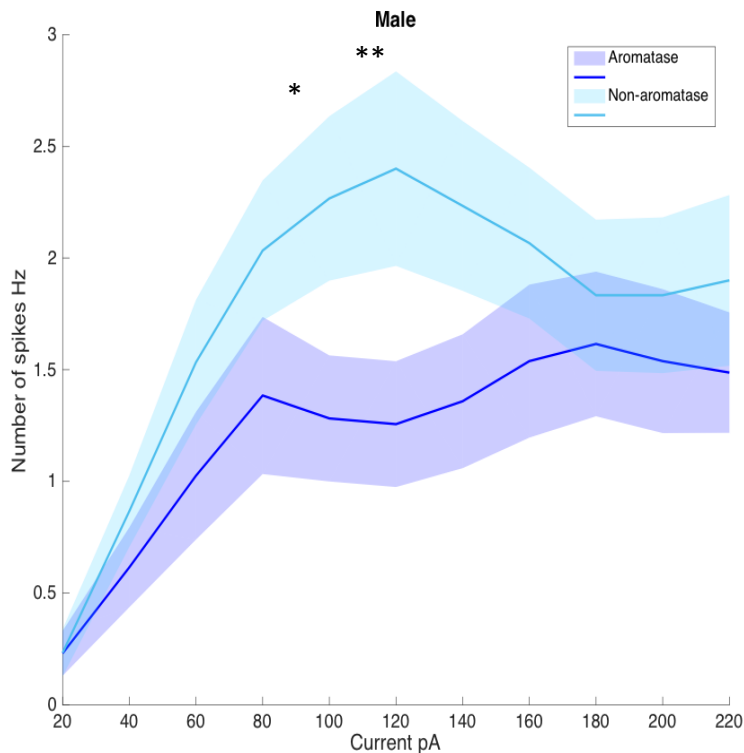


Figure 9. Number of spikes by current in $arom^+$ and $arom^-$ neurons in the MeA male mice. Dark blue trace: number of spikes mean in $arom^+$ neurons; dark blue shading: SEM. Dark cyan: number of spikes mean in $arom^-$ neurons; cyan shading: SEM.

ttest

* $p=0.03$ – ($arom^+$ neurons: mean: 1.282 spikes, SEM= 0.282), ($arom^-$ neurons: mean: 2.266 spikes, SEM= 0.361).

** $p=0.03$ – ($arom^+$ neurons: mean: 1.256 spikes, SEM= 0.281), ($arom^-$ neurons: mean: 2.4 spikes, SEM= 0.427),

3.3 Estradiol activity on $arom^+$ neurons

We tested whether estradiol (E2) could rapidly influence the intrinsic properties of $arom^+$ neurons. All recorded $arom^+$ neurons displayed a clear reduction in firing rates after applying estradiol (Fig. 10 A-B). When estradiol was not applied, the firing pattern in $arom^+$ neurons was stable across time (Fig. 11).

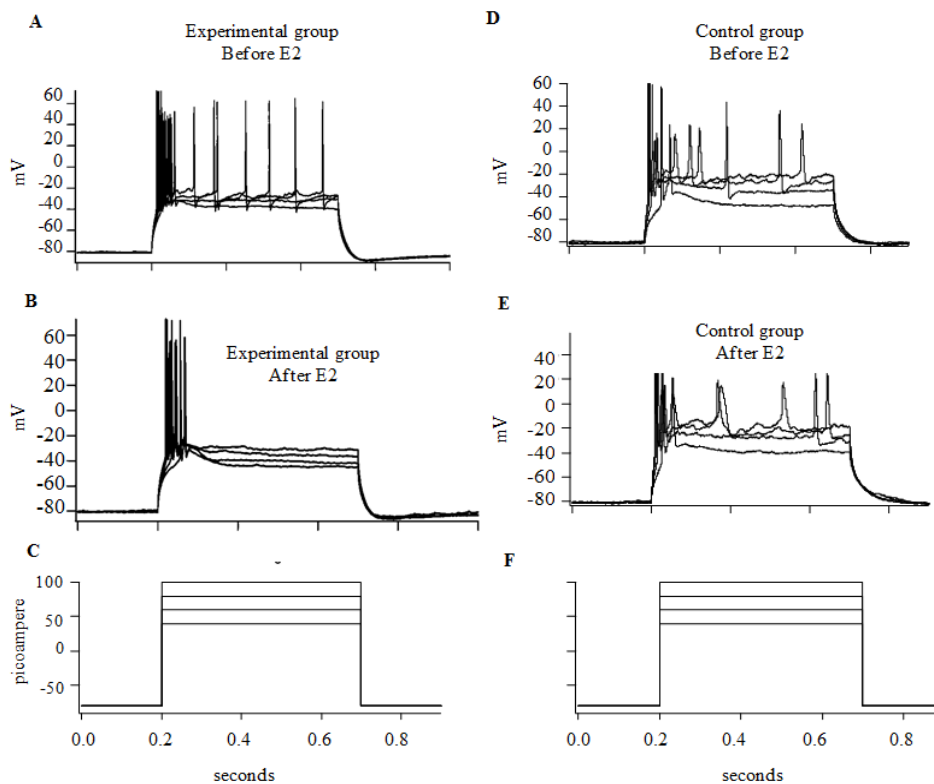


Figure 10. Estradiol activity on $arom^+$ neurons in the MeA in males. A) Firing pattern of $arom^+$ neurons in male before application of estradiol in response to the current step stimulus. B) Firing pattern from the same $arom^+$ neuron as in A, but after 35 minutes of estradiol application. C;F) Current step stimulus - four current steps with an increase of 20pA for each step during 500ms. D;E) Control, with time zero and 35 minutes patching.

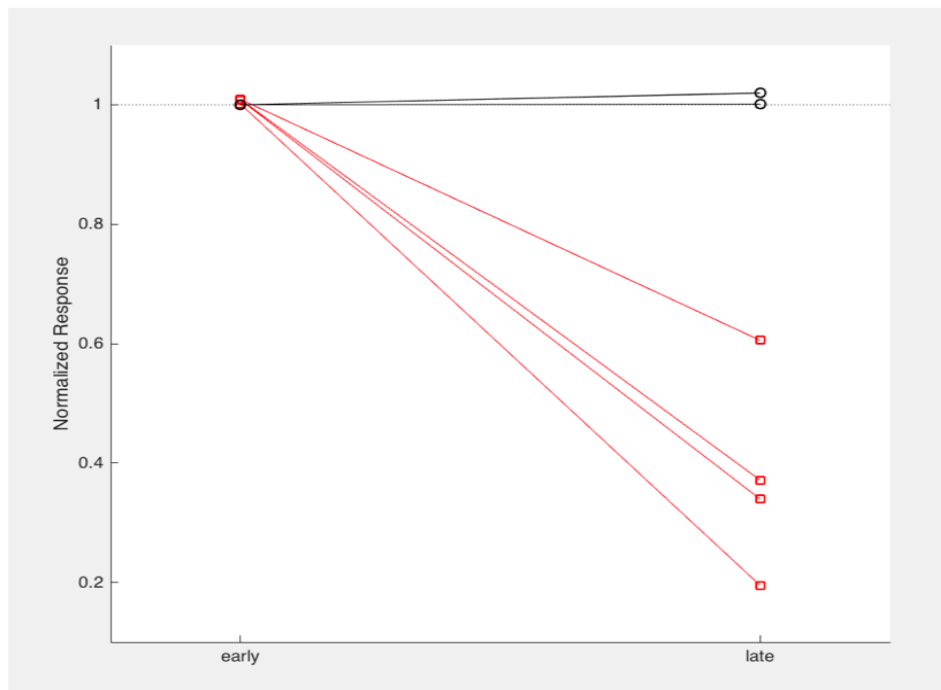


Figure 11. Estradiol activity on $arom^+$ neurons in the MeA across time. Normalized spike frequency response to estradiol + external solution (red line) and external solution only (black line). Early response relates to time zero when the solution is applied. Late response relates to 35 minutes after the solution is applied.

CHAPTER 4

DISCUSSION

Here we describe the intrinsic properties of arom^+ and arom^- neurons in the MeA of male and female mice. Ultimately, the intrinsic properties of neurons control how information is encoded and transmitted through neural circuits. Analyzing the variability of these parameters can help us understand how this circuit can produce different behaviors in male compared to female animals. We demonstrate that the same population of cells (arom^+ neurons) is similar in most of their intrinsic properties in males and females in the MeA. This finding is surprising given the previously established sex-differences in anatomy, sensory representation, and behavioral implication of MeA neurons (Cooke et al., 1999; Morris et. al, 2008; Wu et al., 2009; Bergan et al., 2014; Hong et. al, 2014; Unger, et. al, 2015; Yao et al., 2017).

The relative refractory period was longer in females than in males. The relative refractory period is related to voltage-gated sodium channel inactivation during the repolarization and potassium channels opening. Thus, one explanation for the sex difference is a different composition of channels (likely potassium channels) in male versus female mice. The refractory period controls the interval after which a neuron has fired until it is able to achieve the threshold to produce another action potential. Arom^+ neurons in female have a longer timing to generate this second action potential, suggesting that the second spike need a longer time in order to occur and that in some circumstances male MeA neurons may be able to fire more rapidly than female MeA neurons.

Arom⁺ neurons, in both males and females, typically fired in a phasic manner – i.e. just one action potential was elicited at the beginning of the stimulus regardless of the size of current step (Fig. 9). Most of arom⁻ neurons in the MeA fire tonically in response to large current steps. Thus, arom⁺ neurons from arom⁻ neurons distinguish two functionally distinct groups of MeA neurons. How these differences in intrinsic properties influence the generation of social behavior remains an open question. One possibility is that arom⁺ neurons fire fewer spikes during social behavior—such sparse coding suggests that each spike from an arom⁺ neuron is likely to convey a lot of information.

While our findings indicate many intrinsic properties of arom⁺ neurons in the MeA are similar between male and female mice, our experiments did not address differences in synaptic input to MeA neurons. Anatomical studies have shown that the projection from AOB to arom⁺ neurons in the MeA is more robust in male mice than in female mice (Niemeyer, unpublished data). Thus, it is possible that sex-differences in MeA neurons are not reflected in their intrinsic properties, but rather, in the quantity and magnitude of synaptic inputs they receive (Keshavarzi et al., 2015). Future experiments will be required to characterize synaptic inputs to MeA neurons, and whether this pattern of activity differs between male animals and female animals.

Estradiol is a critical modulator of MeA neural function (Simoni & Yu, 2006; Wu et al., 2009). Given the distinct differences in circulating E2 levels in male and female mice (Amateau et al., 2004; Konkle and McCarthy, 2011), we tested whether the sex steroid E2 altered activity in arom⁺ neurons. Estradiol rapidly reduced the firing rate in all arom⁺ neurons tested. While these results are preliminary, they suggest the possibility that our brain slice preparation underestimates estradiol-dependent sex-differences in responsivity that may be present *in vivo*. Future studies

to confirm if E2 is necessary and/or sufficient to alter intrinsic properties need to be tested in vivo with normal E2 levels.

The Medial amygdala and arom^+ neurons have been repeatedly implicated in establishing sex differences in neuroanatomy and behavior (Cooke et al., 1999; Morris et. al, 2008; Wu et al., 2009; Bergan et al., 2014; Hong et. al, 2014; Unger, et. al, 2015; Yao et al., 2017). Here, we demonstrate that arom^+ neurons in the medial amygdala are surprisingly similar in their intrinsic properties between male and female. Arom^+ neurons respond sparsely to sensory stimuli with phasic firing and slow spiking rates in general. The response to current pulses was similar in arom^+ neurons in both sexes, and the maximum frequency of spikes, the frequency of spikes at the resting membrane potential, the voltage threshold for eliciting an action potential, the timing of action potential initiation and the input resistance of the cell were not significantly different between male and female. On the other hand, after-hyperpolarization differed between sexes, being larger in females, suggesting that different channels composition might be in arom^+ neurons in females and not in males or vice-versa. Additional experiments are needed to identify the sensory conditions during which the observed sex difference in after hyperpolarization limits the maximum achievable firing rate.

In contrast, the differences between arom^+ neurons and arom^- neurons in the MeA were profound. This suggests arom^+ neurons represent a unique subset of cells, interleaved with other MeA populations, but likely playing a unique role in the generation of social behaviors.

BIBLIOGRAPHY

Amateau SK, Alt JJ, Stamps CL and McCarthy MM. Brain estradiol content in newborn rats: sex differences, regional heterogeneity, and possible de novo synthesis by the female telencephalon. *Endocrinology*. 2004.

Balthazart J and Ball GF. Is brain estradiol a hormone or a neuro-transmitter? *Trends Neurosci* 29:241–9. 2006.

Bergan JF, Ben-Shaul Y, Dulac C. Sex-specific processing of social cues in the medial amygdala. *Elife*. 2014. doi: 10.7554/eLife.02743.

Bubenik GA and Brown GM. Morphologic sex differences in primate brain areas involved in regulation of reproductive activity. *Experientia*. 1973.

Choi GB, Dong HW, Murphy AJ, Valenzuela DM, Yancopoulos GD, Swanson LW, Anderson DJ. Lhx6 delineates a pathway mediating innate reproductive behaviors from the amygdala to the hypothalamus. *Neuron*. 2005. doi:10.1016/j.neuron.2005.04.011, pmid:15944132.

Cooke BM, Tabibnia G And Breedlove SM. A brain sexual dimorphism controlled by adult circulating androgens. *Proc. Natl. Acad. Sci. USA*. 1999.

Dielenberg RA, Hunt GE, McGregor IS. “When a rat smells a cat”: the distribution of Fos immunoreactivity in rat brain following exposure to a predatory odor. *Neuroscience*. 2001. Doi: 10.1016/S0306-4522(01)00150-6.

Grenhoff, J, Aston-Jones, G. and Svensson, TH. Nicotinic effects on the firing pattern of midbrain dopamine neurons. *Acta Physiologica Scandinavica*. 1986. doi:10.1111/j.1748-1716.1986.tb07988.x

Hong W, Kim DW and Anderson DJ. Antagonistic control of social behaviors by inhibitory and excitatory neurons in the medial amygdala. *Cell*. 2014. Doi: 10.1016/j.cell.2014.07.049.

Kang N, Baum MJ, Cherry JA. Different profiles of main and accessory olfactory bulb mitral/tufted cell projections revealed in mice using an anterograde tracer and a whole-mount, flattened cortex preparation. *Chem Senses*. 2011. <https://doi.org/10.1093/chemse/bjq120>

Keshavarzi S, Power JM, Albers EH, Sullivan RK, Sah P. Dendritic organization of olfactory inputs to medial amygdala neurons. *J Neurosci*. 2015. doi:10.1523/JNEUROSCI.0627-15.2015 pmid:26400933

Kondo Y. Lesions of the medial amygdala produce severe impairment of copulatory behavior in sexually inexperienced male rats. *Physiology and Behavior*. 1992.

Konkle AT and McCarthy MM. Developmental time course of estradiol, testosterone, and dihydrotestosterone levels in discrete regions of male and female rat brain. *Endocrinology*. 2010.

- Madisen L, Zwingman TA, Sunkin SM, et al. A robust and high-throughput Cre reporting and characterization system for the whole mouse brain. *Nat Neurosci.* 2009. doi: 10.1038/nn.2467
- McKenzie S, Robinson NT, Herrera L, Churchill JC, Eichenbaum H. Learning causes reorganization of neuronal firing patterns to represent related experiences within a hippocampal schema. *J Neurosci.* 2013. Doi: 10.1523/JNEUROSCI.0879-13.2013
- Meredith M, Westberry JM. Distinctive responses in the medial amygdala to same-species and different-species pheromones. *J Neurosci.* 2004. Doi: 10.1523/JNEUROSCI.1139-04.2004.
- Morris JA, Jordan CL, Breedlove SM. Sexual differentiation of the vertebrate nervous system. *Nat Neurosci.* 2004. Doi: 10.1038/nn1325.
- Morris JA, Jordan CL, King ZA, et al. Sexual dimorphism and steroid responsiveness of the posterodorsal medial amygdala in adult mice. *Brain Res.* 2008. doi: 10.1016/j.brainres.2007.11.005.
- Nomoto K and Lima SQ. Enhanced male-evoked responses in the ventromedial hypothalamus of sexually receptive female mice. *Curr Biol.* 2015.
- Numan M, Numan MJ and English JB. Excitotoxic amino acid injections into the medial amygdala facilitate maternal behavior in virgin female rats. *Hormones and Behavior.* 1993.
- Naftolin F, Ryan KJ, Petro Z. Aromatization of androstenedione by the diencephalon. *J Clin Endocrinol Metab.* 1971.
- Naftolin F, Horvath TL, Jakab RL, Leranth C, Harada N and Balthazart J. Aromatase immunoreactivity in axon terminals of the vertebrate brain. An immunocytochemical study on quail, rat, monkey and human tissues. *Neuroendocrinology.* 1996
- Pardo-Bellver C, Cádiz-Moretti B, Novejarque A, Martínez-García F, Lanuza E. Differential efferent projections of the anterior, posteroventral, and posterodorsal subdivisions of the medial amygdala in mice. *Front Neuroanat.* 2012. doi: 10.3389/fnana.2012.00033.
- Paxinos G and Watson C. *The Rat Brain in Stereotaxic Coordinates* (Academic, New York). 1982.
- Remage-Healey L and Bass AH. A rapid neuromodulatory role for steroid hormones in the control of reproductive behavior. *Brain Res.* 2006.
- Remage-Healey L, Maidment NT and Schlinger BA. Forebrain steroid levels fluctuate rapidly during social interactions. *Nat Neurosci.* 2008.
- Sheridan P J. The nucleus interstitialis striae terminalis and the nucleus amygdaloideus medialis: prime targets for androgen in the rat forebrain. *Endocrinology.* 1979.

Simerly RB, Chang C, Muramatsu M, Swanson LW. Distribution of androgen and estrogen receptor mRNA-containing cells in the rat brain: an in situ hybridization study. *J Comp Neurol*. 1990.

Swanson LW. *Brain Maps: Structure of the Rat Brain* (Elsevier, New York). 1992.

Unger EK, Burke KJ Jr, Yang CF, Bender KJ, Fuller PM, Shah NM. Medial amygdalar aromatase neurons regulate aggression in both sexes. *Cell Rep*. 2015. doi: 10.1016/j.celrep.2014.12.040.

Yao S, Bergan J, Lanjuin A, Dulac C. Oxytocin signaling in the medial amygdala is required for sex discrimination of social cues. *Elife*. 2017.

Yokosuka M, Okamura H, Hayashi S. Postnatal development and sex difference in neurons containing estrogen receptor- α immunoreactivity in the preoptic brain, the diencephalon, and the amygdala in the rat. *J Comp Neurol*. 1997. Wu MV, Manoli DS, Fraser EJ, Coats JK, Tollkuhn J, Honda SI, Shah NM. Estrogen masculinizes neural pathways and sex-specific behaviors. *Cell*. 2009.